



TITLE:

LOW DIMENSIONAL CONDUCTORS : A NEW SERIES OF
TRANSITION METAL TETRACHALCOGENIDES (MX₄)_nY (M
= Nb, Ta ; X = S, Se ; Y = halogen) : STRUCTURAL
DETERMINATIONS AND PHYSICAL
PROPERTIES(EXPERIMENTS ON (MX₄)_nY COMPOUNDS,
International Symposium on NONLINEAR TRANSPORT AND
RELATED PHENOMENA IN INORGANIC QUASI ONE
DIMENSIONAL CONDUCTORS)

AUTHOR(S):

MEERSCHAUT, A.

CITATION:

MEERSCHAUT, A.. LOW DIMENSIONAL CONDUCTORS : A NEW SERIES OF TRANSITION METAL TETRACHALCOGENIDES
(MX₄)_nY (M = Nb, Ta ; X = S, Se ; Y = halogen) : STRUCTURAL DETERMINATIONS AND PHYSICAL
PROPERTIES(EXPERIMENTS ON (MX₄)_nY COMPOUNDS, Internation ...

ISSUE DATE:

1984-01-20

URL:

<http://hdl.handle.net/2433/91165>

RIGHT:

LOW DIMENSIONAL CONDUCTORS.

A NEW SERIES OF TRANSITION METAL TETRACHALCOGENIDES

$(MX_4)_nY$ (M = Nb, Ta ; X = S, Se ; Y = halogen) :

STRUCTURAL DETERMINATIONS AND PHYSICAL PROPERTIES.

A. MEERSCHAUT

U.E.R. de Chimie, L.A. 279

2, rue de la Houssinière,

44072 NANTES (France)

- Octobre 1983 -

In studies concerning low-dimensional conductors, the chemist plays an important role. He has to prepare new materials taking in account some structural rules and ionicity structure relationship about the relative stability of atomic fibers or slabs in a given structure. Then he has to look for new polytypes associating in different ways the same slabs or fibers. He can also act upon the lateral bonds which link chains together, thus modifying the real dimensionality of the compounds. Finally, he also has to be concerned with the depinning of C.D.W. because the depinning field is impurity or defect dependent (defects being created by irradiation technique).

In this paper, I would like to illustrate these points with some materials elaborated in our group at NANTES University. I will briefly remind you some aspects concerning trichalcogenides before presenting a new class of materials, the halogened tetrachalcogenides of transition metal $(MX_4)_nY$.

We prepared $NbSe_3$ for the first time in 1975 (1) and found with P. MONCEAU (2) the two CDWs origin of the phase transitions (fig. 1, 2).

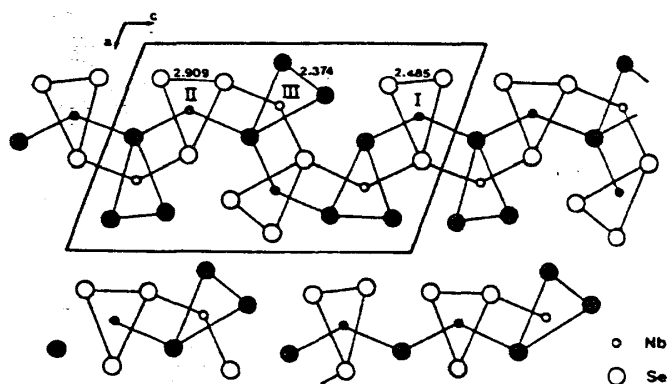


Fig. 1 - Projection along [010] of the monoclinic $NbSe_3$ structure.

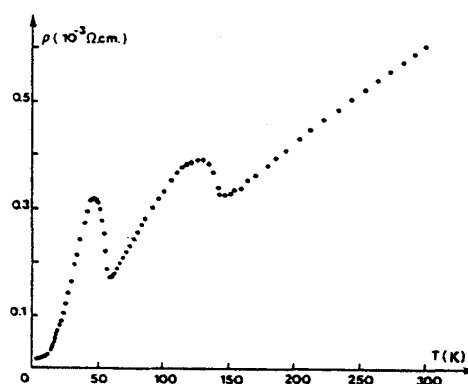


Fig. 2 - Resistivity versus temperature.

Some time later, $NbSe_3$ was found to exhibit a collective charge transport (3) associated with the motion of the C.D.W. (sliding mode) as envisioned by FRÖHLICH in 1954 (4). However the non linear conductivity is only observed above a threshold field, E_T , i.e when the strength of the electrical

field overcomes the pinning force of the C.D.W. on the underlying lattice.

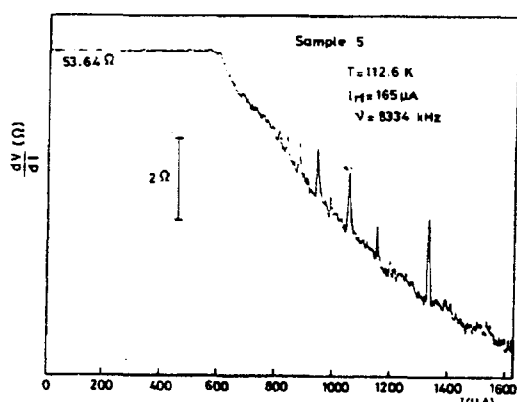


FIG. 3. Differential resistance dV/dI (at 33 Hz) as a function of the current swept in the sample with a 8.334-MHz rf field applied. Peaks indicate synchronization of the noise frequencies with the external frequency.

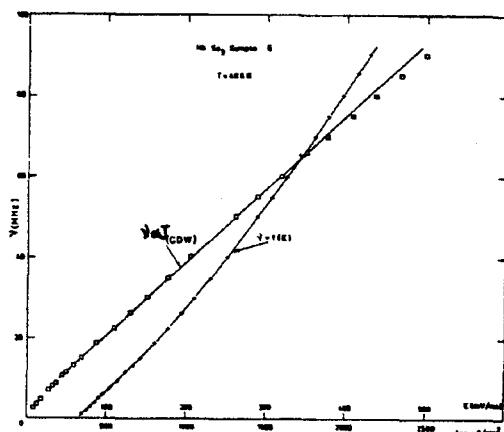


FIG. 4. Variation of the fundamental frequency v_0 as a function of the electric field for large values of E . We have shown also the variation of v as a function of the current carried by the J_{CDW} .

Fig. 3, 4 - From MONCEAU et al. (6).

Grenoble group and GRUNER), in the second one it is due to the motion of discommensurations (BAK). Any of these theories are totally satisfying. We were thus concerned by preparing new materials exhibiting non linear effects to get a better understanding of these intriguing properties.

First of all, polytypism was envisioned since it is frequently observed for the MX_2 series. Pressure studies may also be undertaken. Indeed, the many different chains having the same composition, present in the NbSe_3 structure, indicate a metastable compound. At very high pressure and high temperature we should expect the very symmetrical form of ZrSe_3 with one chain per unit cell for the niobium derivative for example. These studies were widely developed by KIKKAWA et al. (7), and led to new high pressure phases such as NbS_3 and

Above the critical field value, noise is generated in the sample. FLEMING and GRIMES (5) showed that the noise is the superposition of a broad band noise and a periodic noise (fig. 3). The fundamental frequencies characteristics of the periodic noise are assumed to be due to the modulation of the current carried by the C.D.W. in the anharmonic pinning potential, $v \propto J_{CDW}$, (see fig. 4, after MONCEAU et al. (6)).

Many models were proposed to cover the non linear characteristics of such systems. They are divided in two groups. In the first one the extraconductivity is due to the motion of the whole C.D.W. (BARDEEN,

TaSe₃ (monoclinic form). Finally, the interchain coupling which determines the anisotropy of the transport properties can be modified by means of substitution, for example selenium by sulfur. Within the chain, we could assume that other transition metal would exhibit the same trigonal prismatic coordination as Nb in NbSe₃. In this respect, we can mention the Nb_{1-x}Ta_xSe₃ phase reported by SAMBONGI.

These investigations led us to characterize a new variety of TaS₃ (monoclinic form (8)) which presents a more pronounced 1D character than NbSe₃. This is clearly demonstrated by the presence of diffuse lines well above the transition (up to 100 K). (from the thesis of ROUCAU (9)). The presence of such diffuse lines above the static C.D.W. formation results from 1D fluctuations of these CDWs, which means there is no phase coherence between adjacent chains. This is a consequence of a linking between chains weaker than in NbSe₃ because the Ta-S bondings are more ionic than the Nb-Se ones.

When substituting Nb by Fe (Fe_xNb_{1-x}Se₃) a new compound FeNb₃Se₁₀ was reported by HILLENUS et al. (10). Structural determination was

carried out at the same time in our group and at Bell Lab. (11)

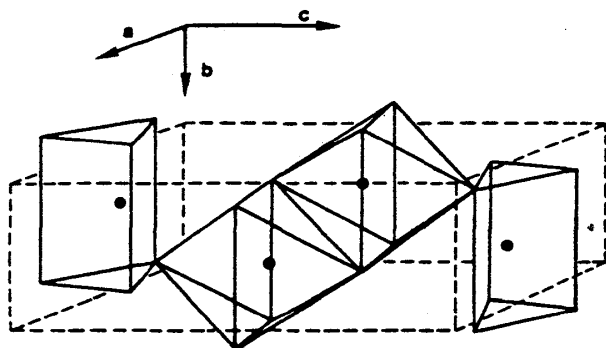
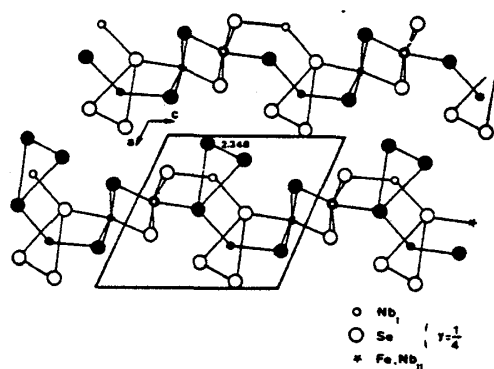


Fig. 5 shows that this compound exhibits two types of chains running in a direction parallel to the b monoclinic axis.

- the first one is a trigonal prismatic chain [NbSe₃] where a C.D.W. develops at low temperature ($T < 140$ K) \vec{q} (0., 0.27, 0.) (10).

- the second one is an octahedral chain in which the disorder of the metal atom

distribution creates a random potential favouring localization of conduction electron associated to an Anderson localization (11).

Fig. 6 a

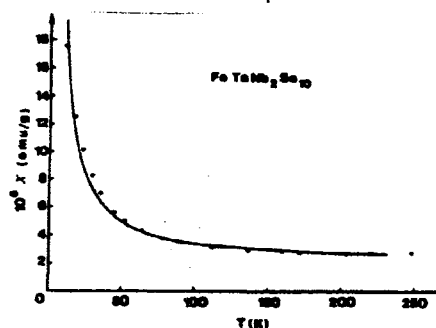
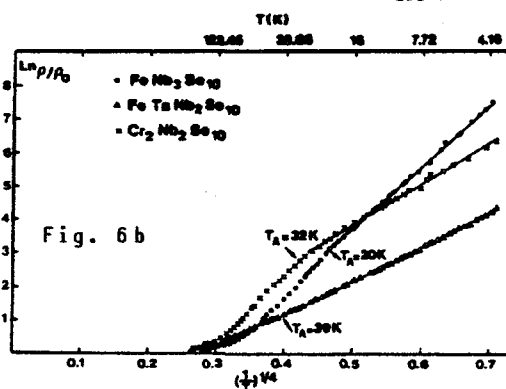
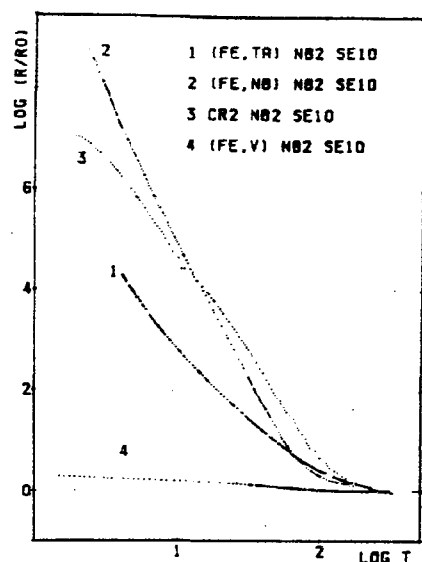
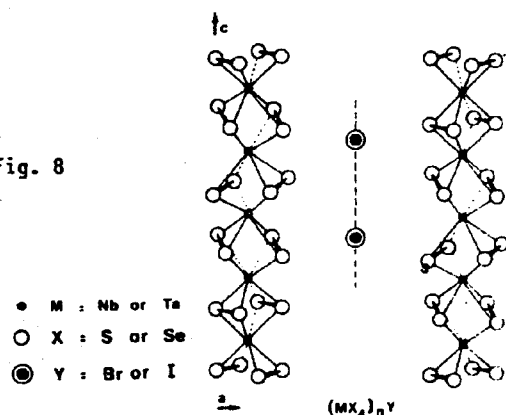


Fig. 8



$FeNb_3Se_{10}$ is the precursor of a new series $(MM')_{OCT}(Nb_2)_TPSe_{10}$ ($MM' = Fe, V, Cr, Ta$) (12). Resistivity behaviors are quite different, see fig. 6a. The resistance rise is about a factor of 10^9 for $FeNb_3Se_{10}$ whereas it is only about 2 for $FeVNb_2Se_{10}$ in the temperature range 140–2 K. Below 40 K, the data are well fitted with a function $\rho \propto \exp T^{-1/4}$ as shown in fig. 6b. This is characteristic of a thermal activated hopping mechanism. The magnetic susceptibility of the Anderson

localized states system has been calculated by SAMBONGI (12) by means of the KOBAYASHI formula (13). Calculated values reproduce very well the experimental data as shown in fig. 7 for the $(FeTa)Nb_2Se_{10}$ case. Curiously, such a series of compounds could not be, up to now, made with sulfur.

Fig. 7

In the chemistry of Nb and Ta chalcogenides, Se pairs begin to appear with the MX_3 formulation. When increasing the amount of chalcogen, and using iodine as transport agent, a new compound $(NbSe_4)_3I$ was characterized in 1977 (14). This compound is the first term of a new series of materials with the general formulation $(MX_4)_nY$ ($M = Nb, Ta$; $X = S, Se$; $Y = Cl, Br, I$ and $n = 2, 3, \dots$) (15). These compounds are built up of $[MX_4]$ chains which are parallel but well separated from one another by halogen atoms, fig. 8, providing a pseudo 1D character to these structures. As for the trichalcogenides, that series of compounds

shows non linear and frequency dependence transport phenomena.

In this talk I shall review only three examples : $(\text{NbSe}_4)_3\text{I}$, $(\text{NbSe}_4)_{10/3}\text{I}$ and $(\text{TaSe}_4)_2\text{I}$

1) $(\text{NbSe}_4)_3\text{I}$

$(\text{NbSe}_4)_3\text{I}$ crystallizes in the tetragonal symmetry with $a = 9.489 \text{ \AA}$, $c = 19.13 \text{ \AA}$, space group $P4/mnc$ (14).

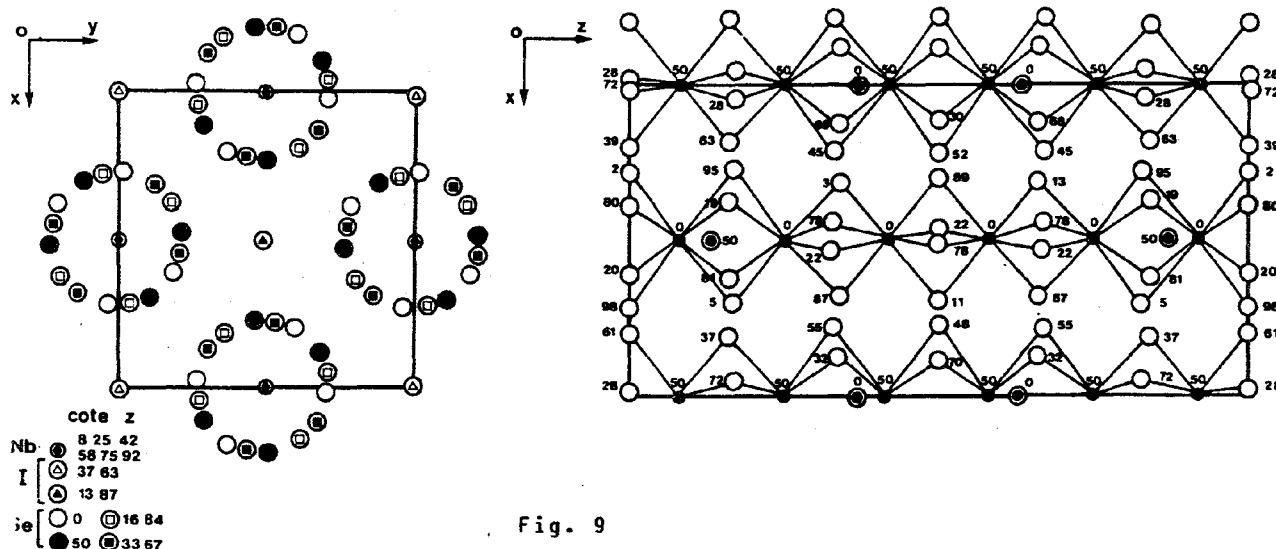


Fig. 9

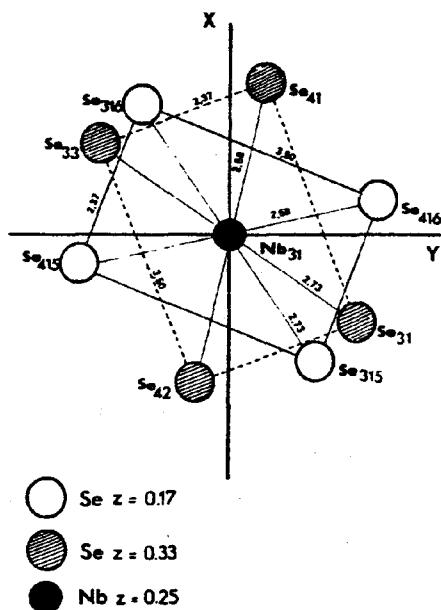


Fig. 10

The structure is composed of $[\text{NbSe}_4]$ chains and iodine columns which are both running parallel to the c axis as can be seen in fig. 9. Niobium atoms are surrounded by eight Se atoms at the corners of a rectangular antiprism. The antiprisms are stacked along the c axis in a screw-like arrangement; two adjacent rectangular $[\text{Se}_4]$ units make a dihedral angle of almost 45° , fig. 10. The dimensions of each rectangle are about 3.5 \AA and 2.35 \AA , the latter value corresponding to the typical $(\text{Se}_2)^{2-}$ pairing. Along the chains, six niobium atoms determine the c periodicity. Two different

Nb-Nb distances (3.06 \AA and 3.25 \AA) occur along the c axis each short Nb-Nb bond being followed by two longer distances. A simple model can be proposed for the niobium sequence. The short Nb-Nb distance could be a consequence of a $\text{Nb}^{4+} - \text{Nb}^{4+}$ bond ($d^1 - d^1$ configuration). These pairs are separated by a Nb^{5+} cation (d^0 configuration) which produces two longer Nb-Nb distances. We thus obtain the ^{formal} charge balance with $2\text{Nb}^{4+} \text{ Nb}^{5+} 6 \text{Se}_2^{2-} \text{I}^-$. Iodine atom has to be considered as I^- in respect to the I-I interatomic distances (4.96 \AA) which is very long as compared to 2.68 \AA in solid I_2 and a maximum of 3.07 \AA in I_3^- .

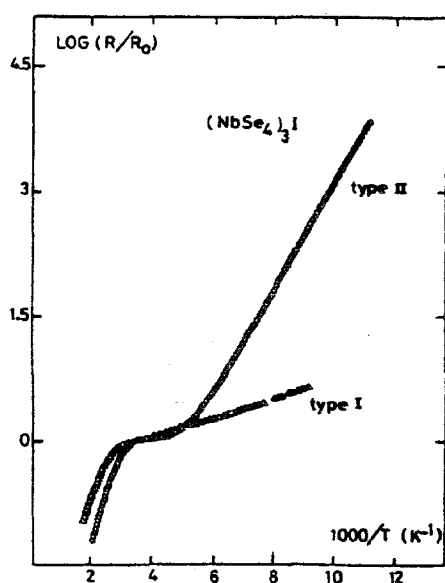


Fig. 11

Such assumptions suggest a semiconducting diamagnetic behavior. Indeed, resistivity measurements indicate semiconducting behavior with a gap of 2200 K above room temperature (15). The slope of the resistivity curve changes below room temperature, and at low temperatures two types of behaviors occur, see fig. 11. At room temperature, both crystal types should be present but could not be distinguished by X-ray techniques. We believe that type II crystal corresponds in fact to an inhomogeneous sample partly constituted with microdomains of $(\text{NbSe}_4)_{10/3} \text{I}$. These domains which act as local defects perpendicularly to the chain axis could be statistically distributed (no X-ray effect)

and are certainly few as we don't observe a significant composition variation within chemical analysis accuracy.

2) $(\text{NbSe}_4)_{10/3} \text{I}$

This new compound exhibits an obvious structural analogy with $(\text{NbSe}_4)_3 \text{I}$ although its structure is more complex, as shown in fig. 12. $(\text{NbSe}_4)_{10/3} \text{I}$ crystallizes in the tetragonal symmetry with $a = 9.464 \text{ \AA}$, $c = 31.910 \text{ \AA}$, space group P4/mcc (16). The a parameter is unaltered as compared to that of previous phase but the c parameter is $10/6$ times that of $(\text{NbSe}_4)_3 \text{I}$ which implies that there are 10 Nb atoms along each $[\text{MX}_4]$ chain in a unit cell. Niobium atoms

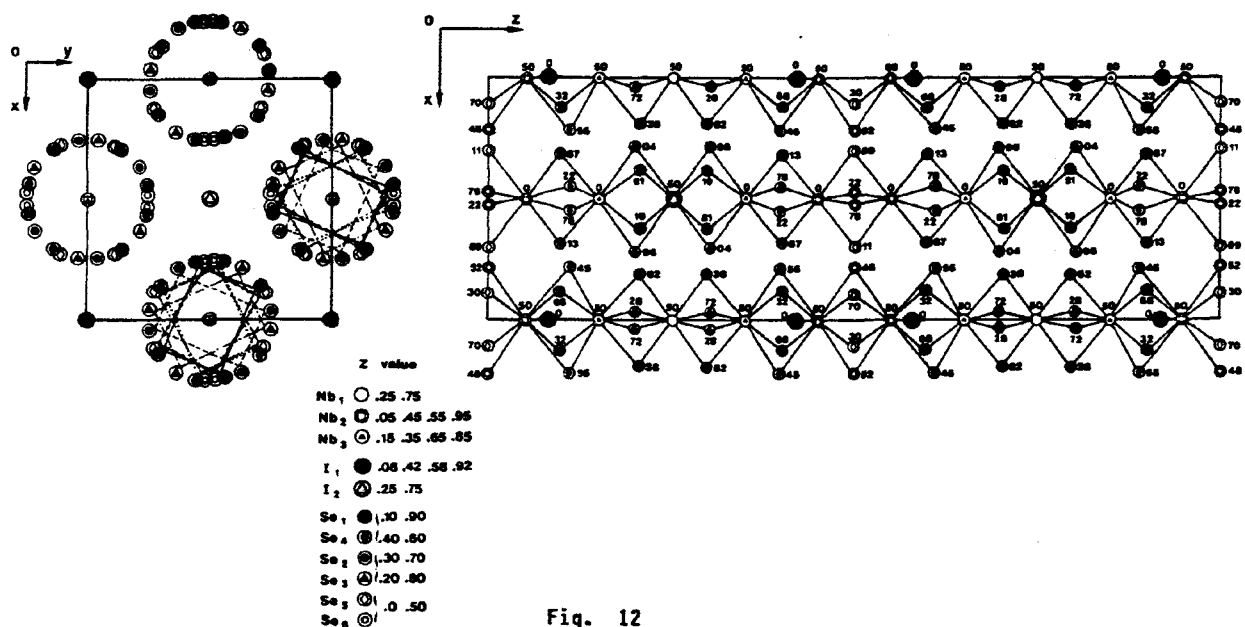


Fig. 12

are not equally distributed within the linear $[MX_4]$ chain. The bond alternation is represented by the following sequence :

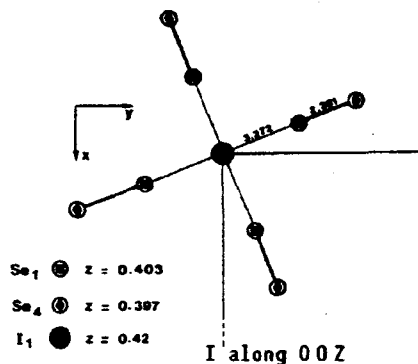
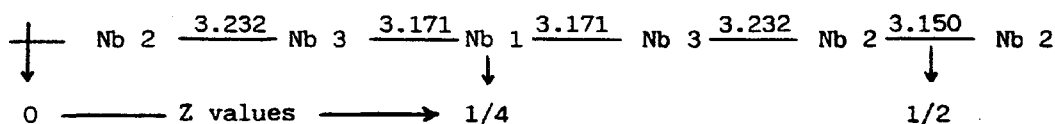


Fig. 13a

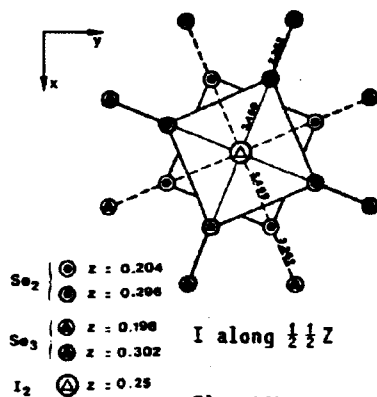
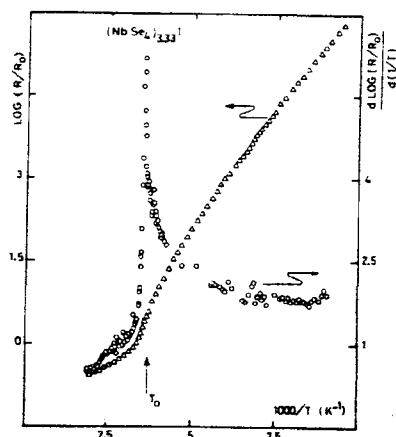


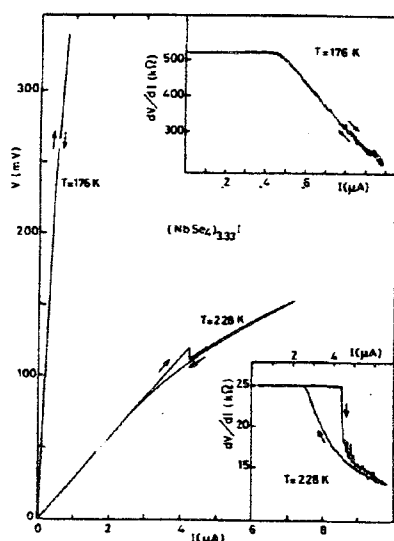
Fig. 13b

The selenium coordination of niobium is also a rectangular antiprism which is composed of four Se_2 pairs. However, the iodine atoms do not show the same distribution within all the channels at is observed for $(\text{NbSe}_4)_3\text{I}$ or $(\text{TaSe}_4)_2\text{I}$. Here in, we can distinguish between two types of channels ; one along the $00z$ axis which is filled by four iodine atoms, the other along the $\frac{1}{2} \frac{1}{2} z$ axis being concerned by only two iodine atoms. In the first case iodine is closely bonded to four selenium atoms (fig. 13a ; $\text{I} - 4 \text{ Se} = 3.272 \text{ \AA}$), while in the second case it is rather weakly bonded to eight selenium atoms (fig. 13b ; $\text{I} - 8 \text{ Se} = 3.469 \text{ \AA}$) in a square antiprismatic arrangement.

The charge transfer from selenium to iodine thus differs in both cases,

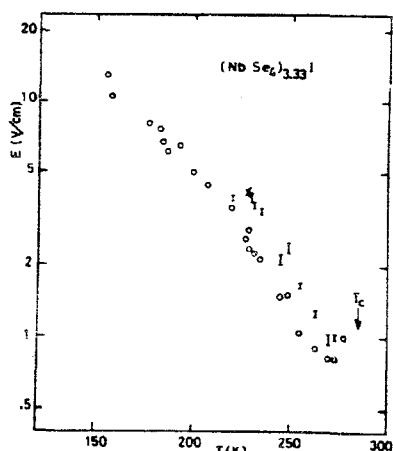


which in turn implies a slightly different electronic charge on the associated niobium atoms. The resistivity variation as a function of temperature, fig. 14, agrees with a thermal activated mechanism ; $\Delta(0) = 3800$ K (17). A phase transition is observed at 285 K as it is clearly shown by a peak in the logarithmic derivative $d \log(R/R_0) / d(1/T)$. The Peierls origin is demonstrated by the appearance of superlattice spots in the electron diffraction pattern (18).



For any temperature below T_0 , the transport properties are non linear (17). This feature is only observed above a threshold field which is determined in the differential resistance curve when dV/dI starts to decrease ; fig. 15. We distinguish two behaviours according to the temperature:

- a) an hysteresis phenomena takes place at the 285 - 220 K temperature range
- b) there is no hysteresis for T below 220 K.



In the first case we are concerned by two threshold fields depending upon the electrical history ; E'_c is the threshold field when E is increased whereas E_c is the threshold field when E is decreased. E_c and E'_c increase exponentially when the temperature is reduced below T_c as it is shown in fig. 16. As for NbSe_3 , noise (i.e broad band noise and periodic noise) is generated in the sample above E_c . These behaviors (non linear conductivity and periodic signals) are strongly indicative

of a charge density wave transport. These phenomena, however, are unobserved for $(\text{NbSe}_4)_3\text{I}$ even under high electric fields of 50 V.cm^{-1} for temperature above 150 K.

3) $(\text{TaSe}_4)_2\text{I}$

Finally a third structural example related to the above ones is given by $(\text{TaSe}_4)_2\text{I}$. $(\text{TaSe}_4)_2\text{I}$ crystallizes in the tetragonal symmetry with $a = 9.531 \text{ \AA}$, $c = 12.824 \text{ \AA}$, space group $\text{I}422$, (19).

The c parameter which is two thirds that of $(\text{NbSe}_4)_3\text{I}$ means that there are four Ta atoms along the chain, fig. 17.

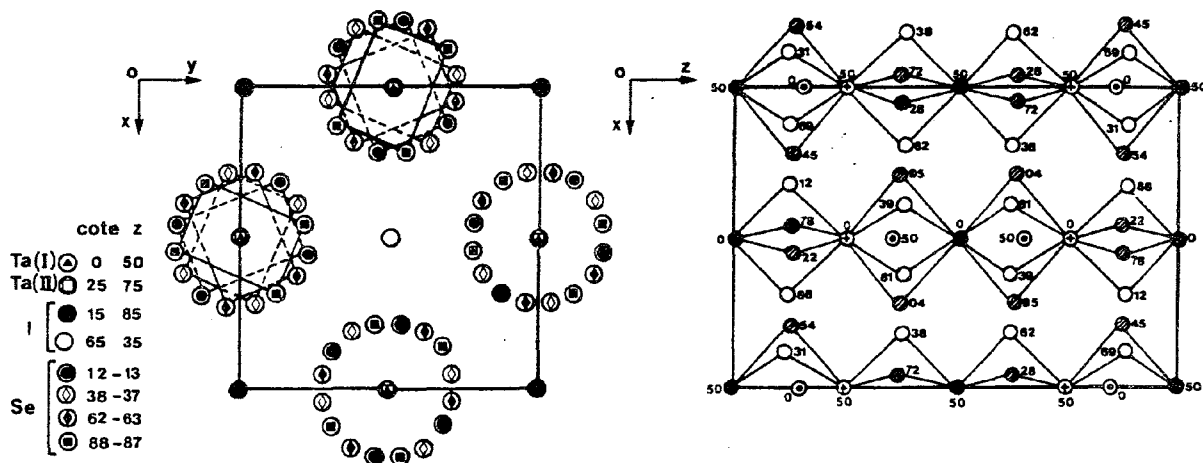


Fig. 17

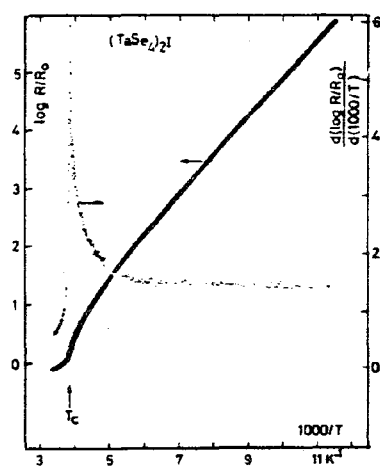


Fig. 18

The Ta-Ta distances within the chain are all identical (3.206 \AA). This is probably the reason why that compound is metallic at room temperature. But, as shown in fig. 18, $(\text{TaSe}_4)_2\text{I}$ undergoes a metal-insulator transition at $T = 263 \text{ K}$ as magnified by the derivative curve. That transition has a C.D.W. origin since superlattice spots have been observed by electron diffraction studies (18). Moreover, $(\text{TaSe}_4)_2\text{I}$ presents non linear properties above a threshold field as

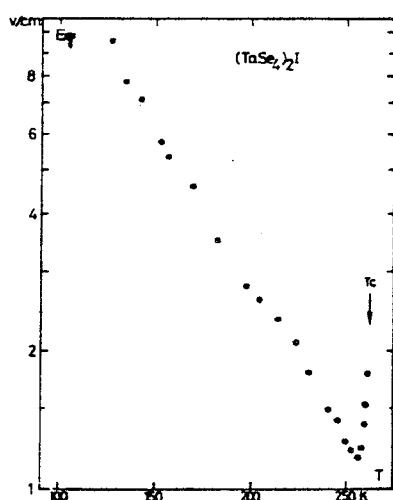


Fig. 19

observed for NbSe_3 and $(\text{NbSe}_4)_{10/3}\text{I}$, which ascertain a Peierls transition for this compound (20, 21). E_T shows an exponential increase below the minimum E_T value (1.2 V.cm^{-1}) when the temperature is reduced (see fig. 19). Once again, noise is generated in the sample when the applied field is greater than E_T , fig. 20 a-b. Fig. 21 shows the variation of the frequency versus the current carried by the C.D.W. (J_{CDW}).

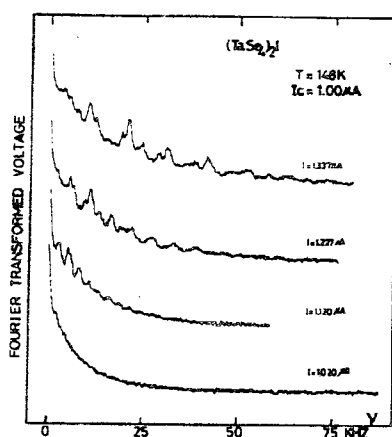


Fig. 20a

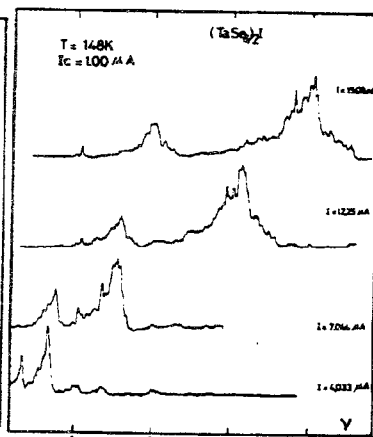


Fig. 20b

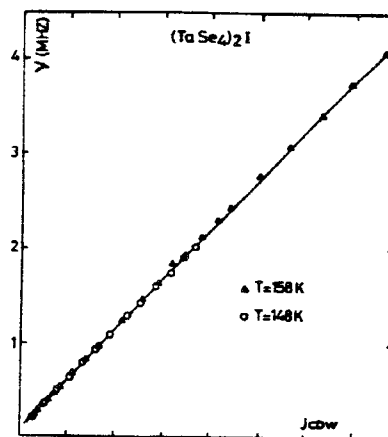


Fig. 21

From these considerations it results that electronic properties of an $[\text{MSe}_4]$ chain are largely determined by the interaction between metal ions along the chain axis. Taking Z axis along the chain, significant interaction between metal ions would occur through overlap between metal d_z^2 orbitals. An average number of d electrons on each metal atom is given by the relation $(n-1)/n$ where n is referred to the index of the chemical formulation $(\text{MSe}_4)_n\text{I}$. As the resulting electrons are localized on a d_z^2 orbital, we may calculate a band filling factor f as : $f = (n-1)/2n$ (22). We then observe that $(\text{NbSe}_4)_3\text{I}$, $(\text{NbSe}_4)_{10/3}\text{I}$ and $(\text{TaSe}_4)_2\text{I}$ would have 1/3, 7/20 and 1/4 filled d_z^2 bands respectively.

A linear chain with incomplete band filling, (i.e. $0 < f < 1$) is a good candidate for a Peierls distortion which opens a band gap at the Fermi level. For a chain with $f < 1/2$, a Peierls distortion increases its repeat distance by a factor of $1/f$. Thus $1/2$, $1/3$ and $1/4$ filled bands are expected to induce lattice dimerization, trimerization and tetramerization.

To summary, the $(MSe_4)_nI$ compounds constitute an exciting series of pseudo 1D materials to study how 1D phenomena such as Peierls distortion and incommensurate CDW formation are affected by band filling. That study was carried out by P. GRESSIER and M.H. WHANBGO (22) who reported molecular and electronic band structure calculations.

A last point which testifies the role of the dz^2 orbital overlaps concerns the resistivity values. These values clearly demonstrate that the highest one (see table I) is referred to the greatest difference between short and long M-M distances.

$(NbSe_4)_3I$	$\rho_{RT} \approx 1. \Omega \text{ cm}$
$(NbSe_4)_{10/3}I$	$\rho_{RT} \approx 1.5 \cdot 10^{-2} \Omega . \text{cm}$
$(TaSe_4)_2I$	$\rho_{RT} \approx 1.5 \cdot 10^{-3} \Omega . \text{cm}$

TABLE I

To finish that review paper, I would like to point out the great similarity (see table II) between the tetrachalcogenide and the blue bronze phases K_xMoO_3 ($x \sim 0.3$) reported by DUMAS and SCHLENKER in this conference.

1)	$K_{0.3}MoO_3 [\equiv (MoO_3)_{10/3}K]$	\longleftrightarrow	$(NbSe_4)_{10/3}I$
	- 10 Octahedra (MoO_3)		10 rectangular antiprisms ($NbSe_4$)
	- CDW phase transition		CDW phase transition
2)	$K_{0.33}MoO_3 [\equiv (MoO_3)_3K]$	\longleftrightarrow	$(NbSe_4)_3I$
	- 6 Octahedra (MoO_3)		6 rectangular antiprisms ($NbSe_4$)
	- semiconductor		semiconductor
<hr/>			
	Alcaline (cation)		Halogen (anion)
	K, Rb, ...		Cl, Br, I

TABLE II

Acknowledgements

I would like to thank J. ROUXEL and P. MONCEAU for their comments. I am grateful to my colleagues P. GRESSIER, A. BEN SALEM and L. GUEMAS who have worked with me on this subject. Thanks also for the contribution of the Grenoble group (P. MONCEAU, M. RENARD, Z.Z. WANG and M.C. SAINT LAGER).

REFERENCES

1. A. MEERSCHAUT and J. ROUXEL, J. Less Comm. Metals 39, 197, (1975).
2. P. MONCEAU, N.P. ONG, A.M. PORTIS, A. MEERSCHAUT and J. ROUXEL, Phys. Rev. Lett. 37, 602, (1976).
3. J. BARDEEN, Phys. Rev. Lett. 42, 1498, (1979).
4. H. FRÖHLICH, Proc. R. Soc. London A223, 296, (1954).
5. R.M. FLEMING and C.C. GRIMES, Phys. Rev. Lett. 42, 1423, (1979).
6. P. MONCEAU, J. RICHARD and M. RENARD, Phys. Rev. B25, 931, (1982).
J. RICHARD, P. MONCEAU and M. RENARD, Phys. Rev. B25, 948, (1982).
7. S. KIKKAWA, N. OGAWA, M. KOIZUMI and Y. ONUKI, J. Sol. St. Chem. 41, 315, (1982).
8. A. MEERSCHAUT, L. GUEMAS and J. ROUXEL, J. Sol. St. Chem. 36, 118, (1981).
9. C. ROUCAU, Thesis, University of TOULOUSE (1981), France.
10. J. HILLENUS, R.V. COLEMAN, R.M. FLEMING and R.J. CAVA, Phys. Rev. B23, 1567, (1981).
11. - A. MEERSCHAUT, P. GRESSIER, L. GUEMAS and J. ROUXEL, Mat. Res. Bull. 16, 1035, (1981).
- R.J. CAVA, V.L. HIMES, A.D. MIGHELL and R.S. ROTH, Phys. Rev. B24, 3634, (1981).
12. A. BEN SALEM, A. MEERSCHAUT, Z.Z. WANG, H. SALVA and T. SAMBONGI, Journal de Physique. submitted.
R.J. CAVA, F.J. DI SALVO, M. EIBSCHUTZ and J.V. WASZCZAK, Phys. Rev. B27 (12), 7412, (1983).
13. S. KOBAYASHI, Y. FUNAGAWA, S. IKEHATA and W. SASAKI, J. Phys. Soc. Jpn 45, 1276, (1978).
14. A. MEERSCHAUT, P. PALVADEAU and J. ROUXEL, J. Sol. St. Chem. 20, 21, (1977).
15. P. GRESSIER, A. MEERSCHAUT, L. GUEMAS, J. ROUXEL and P. MONCEAU, J. Sol. St. Chem. to be published.
16. A. MEERSCHAUT, P. GRESSIER, L. GUEMAS and J. ROUXEL, J. Sol. St. Chem. to be published.
17. Z.Z. WANG, P. MONCEAU, M. RENARD, P. GRESSIER, L. GUEMAS and A. MEERSCHAUT, Sol. St. Comm. 47 (6), 439, (1983).
18. C. ROUCAU and R. AYROLES, private communication.
19. P. GRESSIER, L. GUEMAS and A. MEERSCHAUT, Acta Cryst. B38, 2877, (1982).
20. M. MAKI, M. KAISER, A. ZETTL and G. GRUNER, Sol. St. Comm. 46, 497, (1983).
21. Z.Z. WANG, M.C. SAINT LAGER, P. MONCEAU, M. RENARD, P. GRESSIER, A. MEERSCHAUT, L. GUEMAS and J. ROUXEL, Sol. St. Comm. 46 (4), 325, (1983).
22. P. GRESSIER, M.H. WHANGBO, A. MEERSCHAUT and J. ROUXEL, Inorg. Chem., Submitted.